Dicle University
Journal of Engineering
https://dergipark.org.tr/tr/pub/dumf
duje.dicle.edu.tr

Research Article

Different DC-Link Control Methods with Multilevel Inverter for Low Harmonic and Efficient Power Transfer in Grid-Tied Hydrogen Fuel Cell Systems

Beyzanur GÖNCÜ[1], Ünal YILMAZ[2*]

[1] Harran University Electrical-Electronics Engineering Department, beyzanurgoncu@gmail.com, Orcid No: 0009-0009-0319-0755
[2] Harran University Electrical-Electronics Engineering Department, uyilmaz@harran.edu.tr, Orcid No: 0000-0003-3993-9309

ARTICLE INFO

Article history:

Received 6 May 2023
Received in revised form 13 June 2023
Accepted 14 June 2023
Available online 20 June 2023

Keywords:

PEMFC, DC-Link Control, Multilevel Inverter, Grid-Tied Systems

Doi: 10.24012/dumf.1293293

* Corresponding author

ABSTRACT

In grid-connected power generation systems, dc-link voltage control is needed to prevent energy losses, reduce voltage fluctuations and provide a stable energy flow. In addition, control of the power factor via the voltage source inverter is a process that supports the efficient use of the energy produced. Moreover, keeping the total harmonic distortion (THD) of the current injected into the grid in accordance with IEEE-519 harmonic standards (<5%), will increase the quality of the grid electrical current. In this study, three different methods (cascade pi-based, adaptive neuro fuzzy and artificial neural networks methods) were proposed for dc-link control. In addition, due to its high power factor (PF) and low harmonic distortion performance, a three-level neutral point clamped (NPC) inverter is modeled for grid-tied proton-exchange membrane fuel cells (PEMFC). The rated power of the proposed system is 50 kW and the system was tested under five different operation scenarios. According to the performance results, the THD in the grid current has been reduced from 8.02% to 3.52% compared to traditional methods, dc-link voltage ripple was observed to be around 1V (<1%), and also the power factor regulation performance increased as unity (>0.99).

Introduction

In recent years, increasing technological developments as well as environmental and climatic concerns around the world have led the scientific world to new research in areas such as the use and control of renewable energy sources. Since renewable energy sources are affected by natural phenomena, inevitable performance differences can make power output uncertain and sometimes impossible to use. Considering all these, the PEMFCs are a serious candidate solution, which is highly efficient, noiseless and environmentally friendly as it does not have any moving parts and at the same time providing flexibility in controllable power output [1]. Due to the stated advantages of PEMFCs, there are many existing application areas such as aircraft, spacecraft and automobiles. In addition, especially in recent years, PEMFCs have started to be used in single-phase and three-phase electricity grid integration applications [2], [3]. When the grid-connected power circuit topologies are examined, it is seen that a dc-dc converter is used to regulate the voltage of the dc energy produced by the fuel cells and a power interface unit consisting of dc-ac inverters is used to inject the electrical energy produced as dc into the ac grid. In addition, the total harmonic distortion of the current injected into the grid should be limited to 5% in accordance with IEEE-519 standards. Therefore, the output of dc-ac inverters is equipped with harmonic damping filters (L, LC, LCL etc.) in order to comply with the grid connection standard [4]. Another factor as important as suppressing the harmonic distortion of the current injected into the grid is the control of the active and reactive power injected into the grid. While active power is defined as power capable of doing useful work, reactive power flow adversely affects energy and transmission capacity and can also cause voltage drop. In order to overcome this situation, the power factor should be controlled and the reactive power needs should be adjusted at the distribution level [5].

According to traditional inverter topologies, multi-level inverters consist of cascade submodules that reduce energy losses and electromagnetic interference as it improves waveform quality. Three-level NPC inverters, one of the multi-level inverter topologies, have become interesting because they have low voltage stress in power circuits, lower total harmonic distortion, and high efficiency [6], [7]. The energy obtained from hydrogen fuel cells is converted with the help of a dc-dc converter. Voltage fluctuations and energy losses may occur during this conversion process. Also, the input voltage of the

inverter has to be checked to keep it constant at the specified reference voltage. In this context, for dc-link control, three different control methods (two closed-loop with pi, anfis-based and ann-based) are used in this study. Although pi controller has several advantages such as simple structure and easy implementation, they are known to have a significant time delay problem and poor control performance. On the other hand, while fuzzy logic control is an alternative and effective solution for the analysis of complex, nonlinear and ill-defined systems, artificial neural networks is defined as an intelligent system that has effective advantages such as learning, adaptation, speed. Morover, adaptive neuro-fuzzy inference system technique has taken its place in the literature as a hybrid research alternative that incorporates efficient solution proposals of fuzzy logic and artificial neural network methods [8], [9]. In this study, a three-phase structure is designed for the grid connection of hydrogen fuel cells. Instead of traditional inverters, NPC three-level inverter and three different dc-link control methods are used for dc-link control. Performance analyzes of the proposed system were carried out under different operating conditions, under sudden changing conditions and at different temperatures. The proposed circuit structure consists of power supply (PEM Fuel cell), dc-link, multi-level inverter, LCL harmonic suppression filter, control structures and is presented in Fig.1. in detail. Matlab/Simulink simulation program was used for the analysis and circuit setup of the proposed system.

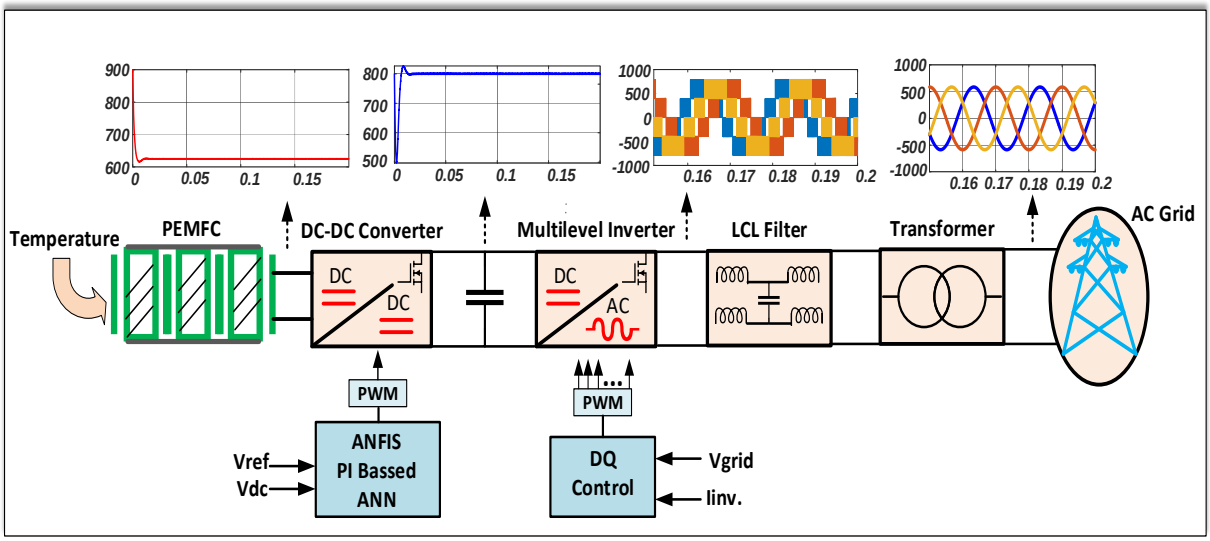

Figure 1. Proposed system for grid-connected PEMFC

Overview of the Literature

Meeting the requirements such as low harmonic distortion, high power factor performance and reactive power balancing, dc-link control, low economic cost, optimization of power circuits as much as possible in order to inject the energy produced by fuel cells into the grid with high efficiency and reliability. When the literature studies are examined, it is seen that studies on fuel cells generally focus on control structures, economical optimization methods, power circuit topologies, and grid failures. Literature studies are detailed in table 1. In ref [10], a multilevel inverter is modeled in order to reduce the number of circuit elements and expand the output voltage level. At the same time, the number of switches has been reduced compared to traditional topologies, thus reducing the switching losses. The total harmonic distortion in the load current was measured as 5.46%. The proposed study has been tested both in a simulated environment and in a laboratory environment. In ref [11], a three-level diode clamped inverter is designed for a multi-stack fuel cell. The aim of the proposed study is to provide energy transfer at low total harmonic distortion level and to reach 85% efficiency. For the proposed study, 1.54 MW/1400 V_{dc} prototype was studied. In Ref [12], an MPPT method is designed to increase the power output by using a FC coupled system ANFIS technique. This designed method provides a significant advantage in reducing the consumption. The proposed FC system was tested with a power rating of 1.9 kW and a dc-dc converter together with an independent system efficiency is 98%.In Ref [13], using the ANFIS method, a concurrently developed control scheme is designed for power transfer between the electrical grid and the battery energy storage system. The proposed scheme allows charging and discharging the battery with bidirectional converter. Simulation studies of the system were carried out on the AC network with a power of 293 W. In Ref [14], a new pulse modulus expansion method with a two-level inverter is proposed. The proposed system provides significant advantages in reducing the harmonics of the inverter connected to the grid, regulating the maximum power output and power factor. In the system, the output current harmonic distortion rate for the two-level inverter is 2.05%, and the harmonic distortion rate for the new PWM scheme is 1.55%.

Table 1. Literature Overview

Subject	Objectives	Rated Power	Energy Source	Ref.
Control Structure	Active reactive power control and low THD	6 kW	PEM Fuel Cell	**[5]**
	Minimize curtailing renewable resources	3.5 MW	SO Fuel Cell	**[15]**
	Active reactive power control and low THD	1.2 MW	Fuel cell	**[16]**
	Improve dynamic voltage response, reduce THD, increase power quality	---	SO Fuel Cell	**[17]**
	Eliminate input current ripple and reduce THD	1.5 kVA	PEM Fuel Cell	**[18]**
	Mathematical solution for grid connected fuel cell	≈8 kW	Fuel cell	**[19]**
	Active reactive power control and THD reduction	6 kW	PEM Fuel Cell	**[20]**
Circuit topology	Modular-Multilevel converter and mitigate THD	6 kW	PEM Fuel Cell	**[21]**
Feasibility	Optimisation for reducing capital and operating expenses	71 kW	SO Fuel Cell/Hybrid	**[22]**
	Optimisation for economic profit	---	Fuel cell vehicle to grid	**[23]**
	Optimisation for economic profit	0.8 kW	SO Fuel Cell/Hybrid	**[24]**
Grid Failures	Maximum power extraction method that also performs in case of grid failure mode	≈ 25kW	PEM Fuel Cell	**[25]**
Both control structure and Circuit topology	dc-link Control, active&reactive power control and low THD	50 kW	PEM Fuel Cell	**Proposed**

Some of the important issues that fuel cells must overcome in order to inject energy into the grid accurately and reliably are the elimination of reactive power and low total harmonic distortion (must comply with IEEE-519 standards). The proposed study consists of two stages. In the first stage, the voltage of the dc energy obtained from PEMFC is increased to the determined reference value with the help of dc-dc converter. In addition, it is controlled by three different dc-link control methods in order to prevent voltage fluctuations and to provide an efficient energy flow. In the second stage, dc energy is converted to ac energy with the help of multi-level inverter. This conversion process; In order to have low harmonic distortion and high power factor, dq- control method is used. Finally, the LCL harmonic suppression filter was designed and energy was supplied to the electricity grid. The three-phase system model is designed with control structures to inject the energy from PEMFCs into the grid. Instead of the traditional inverter model and pi-based dc link control method, a multi-level inverter and three different dc link control algorithms are designed. Thanks to the proposed system, it has been determined that the suppression performance of the current harmonics injected into the grid and the power factor regulation are improved compared to the traditional method. In this case, the energy injected into the grid is more efficient and of higher quality. In order to ensure low voltage fluctuation and efficient energy flow, three different methods have been applied for DC-link control: ANFIS-based, ANN-based and two closed-loop pi-based. The purpose of applying these methods is to perform performance analysis of traditional methods (pi-based) and intelligent methods (ANFIS and ANN-based). To confirm the accuracy of the proposed system and control methods have been tested under different and suddenly changing operating conditions and performance analysis has been carried out under different temperatures. LCL Harmonic suppression filter is designed and applied to the output of the NPC three-level inverter in order to prevent possible electrical faults and to improve the electrical quality.

Material and Methods

Before injecting the dc energy produced by the fuel cells into the grid, power electronics interface circuits are needed. They consist of a dc-dc converter to control the input voltage level of the inverter and then an inverter to convert dc energy to ac energy. Finally, a filter circuit is needed to perform harmonic suppression between the inverter and the grid.

Fuel Cell Stack and DC-Link Control

Fuel Cells are devices that convert the chemical energy they contain into dc electrical energy as a result of electrochemical reactions. Considering its low noise, high power density, high efficiency and low pollution, PEMFC has become one of the most popular fuel cells [16]. The equivalent circuit of the PEM fuel cell is shown in Fig. 2 [2].

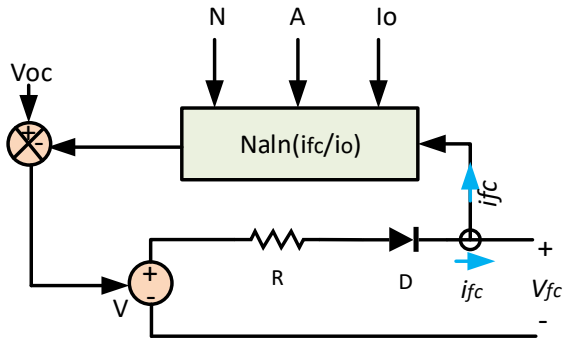

Figure 2. Electrical circuit equivalent of a PEM fuel cell

The voltage value produced by the fuel cell can be found by following expression.

$$.V_{fc} = V_{oc} - V_R - V_d \quad (1)$$

The open-circuit voltage can be found from the following equation.

$$V_{oc} = K_C \left[V_o + (T - 298)\frac{-44{,}43}{zF} + \frac{R_C T}{zF} \ln\left(PH_2 PO_2^{1/2}\right)\right] \quad (2)$$

Resistive and the absolute polarization overvoltages can be calculated with the following equations.

$$\left\{\begin{matrix} V_R = i_{FC} \times R \\ V_d = N \times A \times \ln\left(i_{FC}/i_O\right) \end{matrix}\right\} \quad (3)$$

If the expressions in the above equations are defined; V_{fc} is the output voltage of the fuel cell, V_R is the voltage loss on the resistor, V_d is the absolute polarization voltage loss, N is the number of cells in the fuel cell, A is the tafel slope and i_o is the current exchange [2].The number of cells used in this study was determined as N=900, rated voltage 625 V and rated power 50kW. The current, voltage and power characteristics of the fuel cell used in this study and the relationship between each other are presented in Fig. 3.

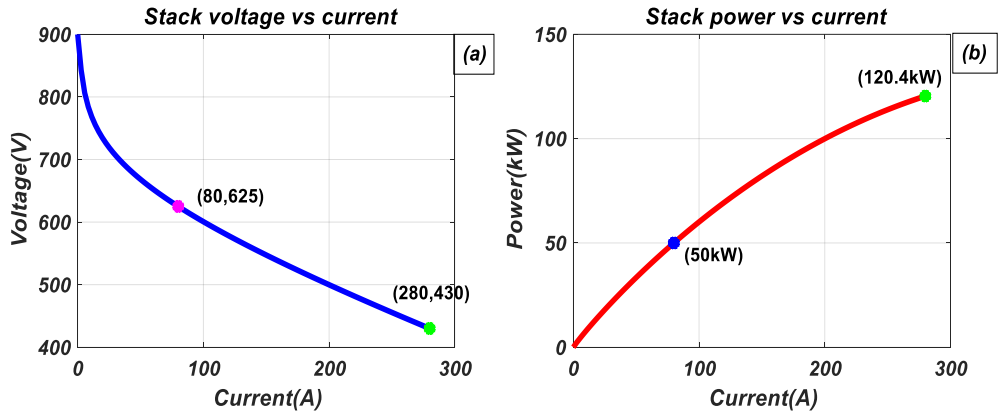

Figure 3. PEMFC Characteristic Curves

The electrical properties and characteristic values of PEMFC used as an energy source are presented in Table 2.

Table 2. PEMFC electrical characteristics.

PEMFC Fuel Cell Model and Operating Properties	
Matlab Model	**PEMFC-50kW-625Vdc**
Current at nominal operating point (A)	80 A
Voltage at nominal operating point (V)	625 V
Current at maximum operating point (A)	280 A
Voltage at maximum operating point (V)	430 A
Fuel cell nominal power (W)	50 kW
Fuel cell maximum power (W)	120.4 kW
Fuel cell resistance (Ω)	0.664 Ω
Number of Cells	900
Nominal stack efficiency (%)	55%
Operating temperature (°C)	65°-70°
Nominal air flow rate (lpm)	2100 lpm
Maximum air flow rate (lpm)	7350 lpm
Fuel nominal supply pressure (bar)	1.5 Bar
Air nominal supply pressure (bar)	1 Bar
Nominal fuel consumption (slpm)	501.8 (slpm)
Nominal air consumption (slpm)	1194 (slpm)

Since the dc energy produced by fuel cells depends on many parameters, connecting it directly to the inverter may cause voltage drops and irregular energy flow. Therefore, as shown in Fig. 4, a dc-dc converter is used between the inverter and the fuel cell. Due to the low number of circuit elements, easy installation, effective and efficient operation, dc-dc boost converter was used in this study. The rated voltage of the fuel cell, 625V, was applied three different dc-link controlled dc-dc boost converters to keep the output at 800V and to feed the input of the NPC multi-level inverter.

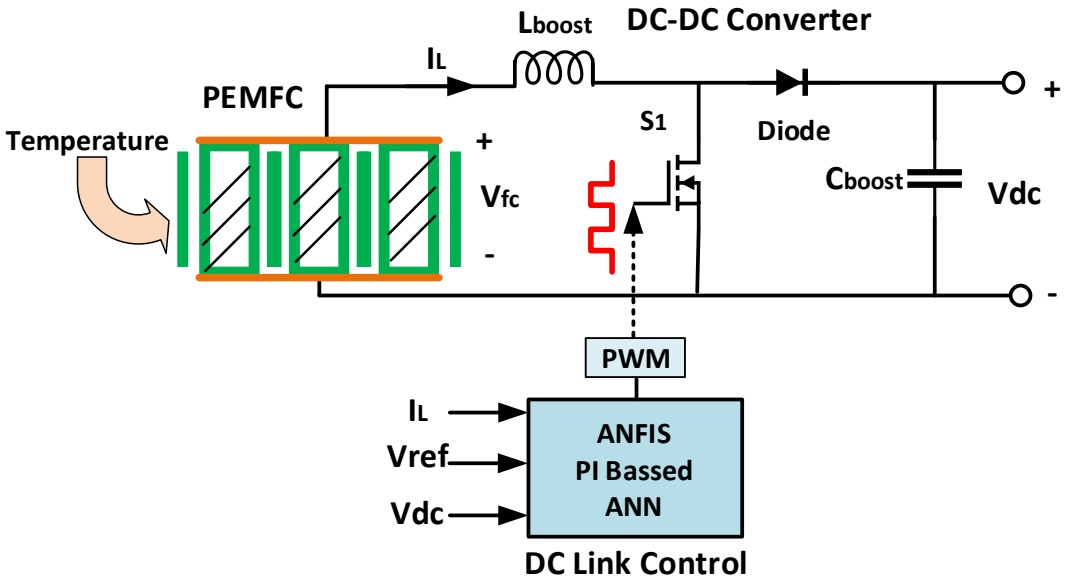

Figure 4. DC Link Control Methods

The relationship between the output voltage of the boost converter and the voltage of the fuel cell is presented below.

$$\frac{V_{dc}}{V_{fc}} = \frac{1}{1-D} \quad (4)$$

$$L_{boost} = \frac{V_{fc}D}{\Delta i_L f_s} \quad (5)$$

$$C_{boost} = \frac{D}{R(\Delta V_{dc}/V_{dc})f} \quad (6)$$

V_{boost} is the output voltage of the dc-dc boost converter, and V_{fc} is the fuel cell voltage, and D is expressed as the duty-cycle of the PWM signal feeding the gate of the semiconductor switch (IGBT).

ANFIS Based DC Link Control

ANFIS-based control structure has been designed for current control after dq conversion and consists of 5 different layers. The ANFIS-based control structure is shown in Fig. 5.

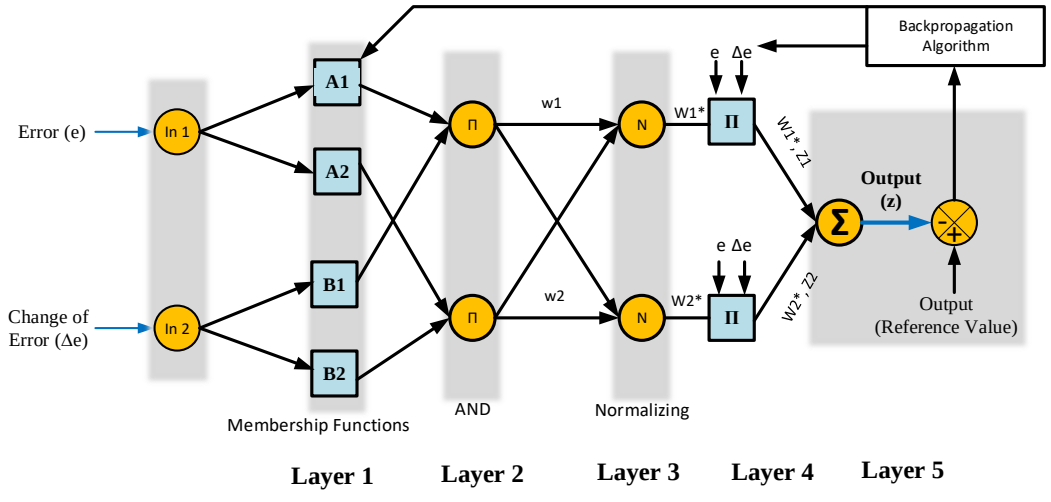

Figure 5. Adaptive Neuro Fuzzy Inference System Structure

ANFIS-based control system is designed to generate duty cycle of pwm signal at the output. Accordingly, the error between the voltages (V_{dcref}-V_{dcLink}) and the rate of change of the error according to time (d(V_{dcref}-V_{dcLink})/dt)) are given to the input of ANFIS.

$$\begin{Bmatrix} e(t) = V_{dc}(ref) - Vdc_{Link} \\ \Delta e(t) = d(V_{dc}(ref) - Vdc_{Link})/dt \end{Bmatrix} \quad (7)$$

Layer 1: In this layer, membership degrees are generated for the input vectors (ai). (i=1,2,3.)

$$Q_i^1 \rightarrow \mu_{Ai}(e) \begin{cases} 0 & e \le ai \\ \frac{e-ai}{bi-ai} & ai \le e \le bi \\ \frac{ei-e}{ei-bi} & bi \le e \le ei \\ 0 & ei \le e \end{cases} \quad (8)$$

Layer 2: Three membership functions are created for each input, and a total of 3x3=9 different rules are created. The properties of the input and output membership functions are shown in Fig. 6 (NB means negative, ZE means zero and PB means positive) [26], [27].

$$Q_i^2 \rightarrow W_i = \min(\mu_{Ai}(e) \cdot \mu_{Bi}(e)) \quad (9)$$

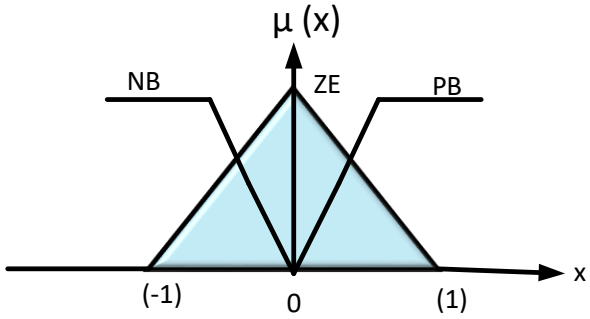

Figure 6. Input and output membership function

Layer 3: In this layer, the ratio of the activation level of each rule to all activation levels is calculated.

$$Q_i^3 \rightarrow \overline{W_i} = \frac{W}{\sum_{J=1}^{N} W_J} \quad (10)$$

Layer 4: In this layer, the contribution of each layer to the total output is calculated with the following function.

$$Q_i^4 = \overline{\overline{W}}_i Z_i = \overline{\overline{W}}_i (k_i e + m_i \Delta e + s_i) \quad (11)$$

Layer 5: In this layer, the sum of the contribution of all rules is calculated.

$$Q_i^5 = \sum_{i=1}^{2} \overline{\overline{W}}_i Z_i = \frac{W_1 Z_1 + W_2 Z_2}{W_1 + W_2} \quad (12)$$

If the expressions in the above equations are defined; e represents error, Δe error rate of change with time, N data number, k, m and s design parameters, w weights, z output, μ(X) membership function and Q represents layers [26], [27].

ANN Based DC Link Control

In this study, an artificial neural network model is designed to control the dc link voltage. Input layer; It consists of reference voltage (Vref) and dc link (Vdc Link) voltage, while the duty cycle is produced for the PWM signal in the output layer. A hidden layer with 10 neurons is designed between the input layer and the output layer. The designed artificial neural network is presented in detail in Fig. 7 [28].

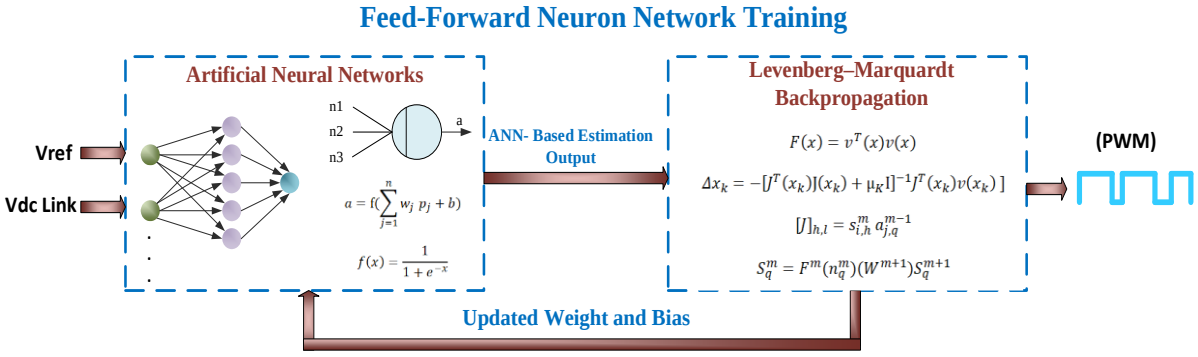

Figure 7. Feed forward artificial neural networks structure

The basic element of artificial neural networks can be defined as mathematically and logically modeling the functions of biological neurons. The input layer vector of the designed neuron is p = [p1, p2, . . . , pR], and w1, w2, .. wj are weighted by the elements of the W weight matrix, respectively. The neuron has bias (b), which is arranged by adding up with the weighted inputs of the neuron, forming the net inputs of n [29].

$$n = \sum_{j=1}^{R} w_j p_j + p = W_p + b \quad (13)$$

After the input layer is weighted and added with bias, it is passed through the activation function.

$$a = f(n) \quad (14)$$

The tan-sigmoid activation function was used for this study and is presented as follows.

$$f = \frac{1}{1+e^{-x}} \quad (15)$$

The following data creation software in matlab simulation program to generate input and target dataset for DC link control

Matlab Dataset Codes

```
Vinput=randi([400 10 650], 1, 100000);
Voutput=randi([650 10 900], 1, 100000);
Duty=(Voutput-Vinput)./Voutput;
İnput=[Vinput;Voutput];
Output=Duty;
```

Two Closed Loop pi-based DC Link Control

In this study, pi-based dc-link control method with two closed loops was used. In this control method, three parameters, dc-link voltage, reference voltage value and inductance current, are used. The error rate is found by taking the difference between the reference voltage and the dc link voltage, then the reference current for the inductance current is found by passing the pi control. The error rate is found by taking the difference between the reference current and the inductance current, and the duty cycle of the pwm signal to be produced is determined by passing this error rate again through the pi control. Finally, the determined duty cycle is compared with a triangular signal and the pwm signal is generated for the switching element. It is detailed in Fig. 8.

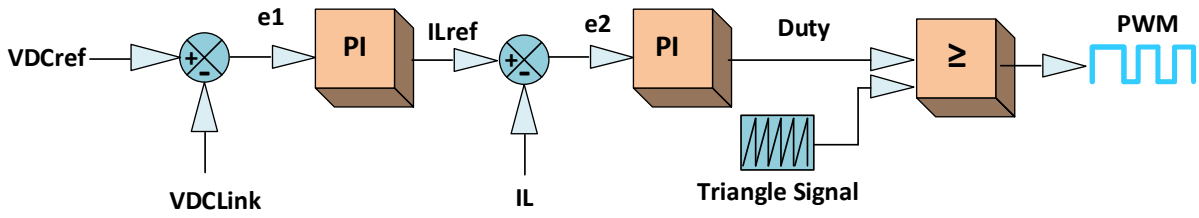

Figure 8. Two closed loop dc link control methods based on PI

Expressed mathematically, the first pi control establishes the reference value for the inductance current [30], [31], [32].

$$I_{Lref} = K_{p1}e_1 + K_{i1}\int e_1 dt \quad (16)$$

Where;

$$e_1 = V_{DCref} - V_{DClink} \quad (17)$$

I_{Lref} can be defined with the following expression.

$$I_{Lref} = \frac{{V_{DCref}}^2}{RV_{FC}} \quad (18)$$

The error rate for the second closed loop is expressed by the following equation.

$$e_2 = K_{p2}e_2 + K_{i2}\int e_2 dt \quad (19)$$

Where;

$$e_1 = I_{Lref} - I_L \quad (20)$$

If the parameters given in the equations are defined, e_1 is the first closed loop error rate, e_2 is the second closed loop error rate, I_{Lref} inductance current reference value, V_{DCLink} dc link voltage, V_{DCref}, dc link reference voltage, I_L inductance current, V_{FC} fuel cell voltage.

Three Level NPC Inverter with Control method

After the dc energy produced by PEMFC is controlled by the dc-dc boost converter and given to the dc-link, this dc energy is used as the input voltage of the NPC three-level inverter. The designed inverter and LCL filter convert dc energy into ac energy to inject it into the grid at low harmonic level. Active reactive power control is performed by synchronizing the grid current and voltage and the signals generated from the inverter output with the dq-based control method. The designed NPC three-level converter LCL filter and dq-based control method are presented in Fig. 9.

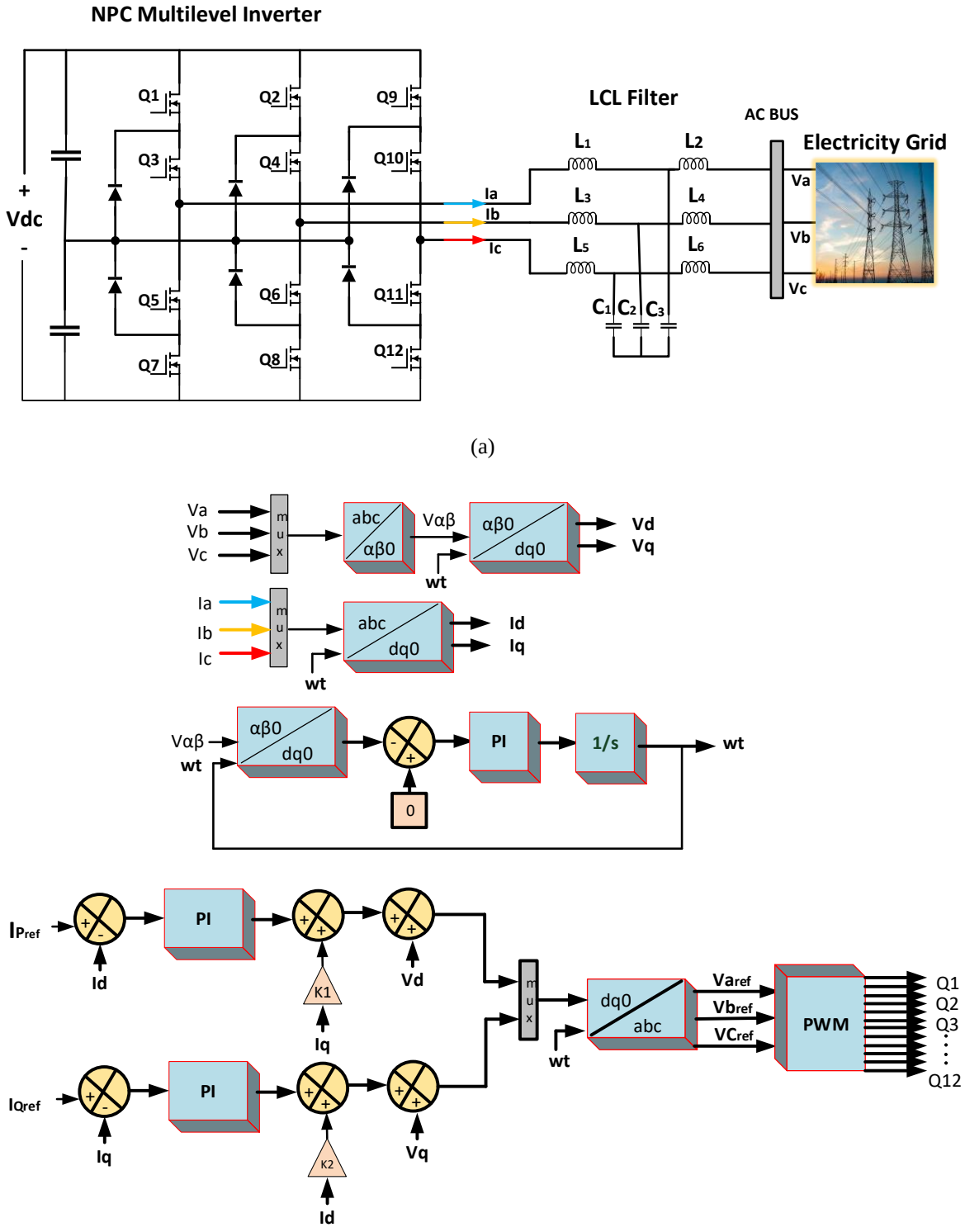

Figure 9. Designed NPC Three-Level Inverter (a) DQ based Control Method (b)

The following procedures should be followed to determine the current and voltage equations of the grid-connected NPC three-level inverter and the dq conversion equations of the three-phase system [6], [33]-[34].

Voltage equations can be written as;

$$\left\{\begin{vmatrix} u_a = Ucos(wt) \\ u_b = Ucos(wt - {}^{2\pi}/_{3}) \\ u_c = Ucos(wt + {}^{2\pi}/_{3}) \end{vmatrix}\right\} \quad (21)$$

If the dq rotating frame is applied as the transform method in the three-phase system (abc), the following equation can be written (The x's in the equation can be thought of as current or voltage.). abc→dq transform [6], [33]-[34];

$$\begin{bmatrix} X_d \\ X_q \end{bmatrix} = \sqrt{\frac{2}{3}} \begin{bmatrix} Coswt & -Sinwt \\ Cos(wt-120^0) & -Sin(wt-120^0) \\ Cos(wt+120^0) & -Sin(wt+120^0) \end{bmatrix}^T \begin{bmatrix} X_a \\ X_b \\ X_c \end{bmatrix} \quad (22)$$

The current equations can be written as:

$$i_d = \sqrt{\frac{2}{3}}(i_a Coswt + i_b Cos(wt-120^0) + i_c Cos(wt+120^0)) \quad (23)$$

$$i_q = -\sqrt{\frac{2}{3}}(i_a Sinwt + i_b Sin(wt-120^0) + i_c Sin(wt+120^0)) \quad (24)$$

Similarly, the voltage equations can be written as:

$$V_d = \sqrt{\frac{2}{3}}(V_a Coswt + V_b Cos(wt-120^0) + V_c Cos(wt+120^0)) \quad (25)$$

$$V_q = -\sqrt{\frac{2}{3}}(V_a Sinwt + V_b Sin(wt-120^0) + V_c Sin(wt+120^0)) \quad (26)$$

For the grid connection of the three-phase system after the ANFIS controller, instead of the previous abc→dq conversion, dq→abc conversion is required to generate reference voltages. Therefore, the following equation is used for the conversion process.

$$\begin{bmatrix} X_a \\ X_b \\ X_c \end{bmatrix} = \sqrt{\frac{2}{3}} \begin{bmatrix} Coswt & -Sinwt \\ Cos(wt-120^0) & -Sin(wt-120^0) \\ Cos(wt+120^0) & -Sin(wt+120^0) \end{bmatrix} \begin{bmatrix} X_d \\ X_q \end{bmatrix} \quad (27)$$

After the three-phase reference voltages (Varef, Vbref, Vcref) are produced, the control process is completed by generating PWM signals for the semiconductor switching elements (IGBT) of the NPC three-level inverter by comparing them with the frequency determined sawtooth signal.

LCL Filter Design

An LCL filter is designed between the three-level NPC inverter and the grid to suppress current harmonics. The equivalent circuit of the three-phase filter designed for each phase is presented in Fig. 10.

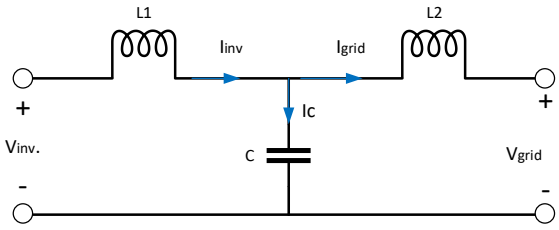

Figure 10. LCL Filter equivalent Circuit

The transfer function between the grid current and the inverter voltage is expressed in the following equation [35].

$$\frac{I_g(s)}{V_{inv}(s)} = \frac{1}{L_1 L_2 C s^3 + (L_2 + L_1)s} \quad (28)$$

In this study, it was calculated as L_1=L_2=500μH, C=100μF. The dynamic response of frequency, magnitude and phase according to the inductor and Fig. 11.

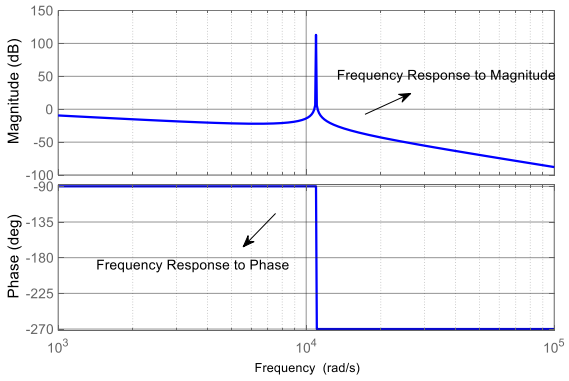

Figure 11. Bode Diagram of LCL filter

The electrical characteristics and circuit parameters of the designed system are presented in Table 3.

Table 3. Circuit Parameters and electrical characteristics.

Parameters	Values
P_{rated}	50 kW
V_{fuel}	625 Vdc
V_{dclink}	800 Vdc
fs	20 kHz
K_{p1}	0.9
K_{i1}	5
K_{p2}	0.02
K_{i2}	5
f	50 Hz
L_{boost}	1.07 mH
C_{boost}	20 mF
L_{1filt}	500 μH
C_{filt}	100 μF
L_{2filt}	500 μH
T_{fuel}	65ºC-70 ºC

Results and Discussion

In this study, 5 different operating conditions were modeled to confirm the accuracy of the proposed system and detailed analysis was performed in all operating conditions. 50kw, 625V PEMFC matlab model was used as energy source in the study. In the first operating condition, no reactive power was requested to the grid and only active power was tried to be injected. In this operating condition, the phase angle between the mains current and voltage is measured as 2.7^0 and the power factor is >0.99. In the second operating condition, the active power demand was reduced abruptly and it was expected that reactive power would not be injected into the grid. In this operating condition, the phase angle is measured as 2.09^0 and the power factor is >0.99. In the third operating condition, active power was kept constant and reactive power was expected to be injected into the grid. In this condition, the phase angle was measured as 11.1^0 and the power factor as >0.98. In the fourth operating condition, more reactive power is expected to be injected into the grid by keeping the active power constant. In this operating condition, the phase angle was measured as 21.12^0 and the power factor was measured as >0.93. In the fifth operating condition, it was expected that the work would suddenly return to its initial state. In this operating condition, the phase angle is measured as 2.7^0 and the power factor is >0.99. Three mains currents in five different situations are presented in Fig. 12.

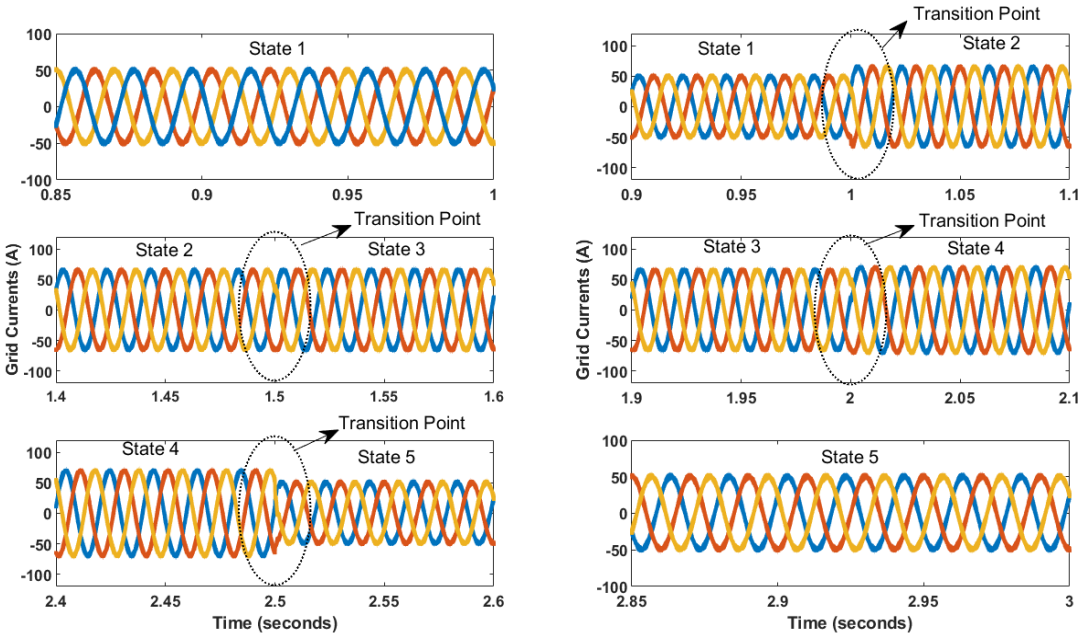

Figure 12. Grid Current under five different operating States

The performances of dc link control methods on power factor were compared under five different operating conditions. The order of convergence times from best to worst: two closed-loop-based, ann-based, and ampis-based. The effects of different dc link control methods on power factor are presented in Fig. 13. In the system designed using dc link control methods and three-level NPC inverter in five different situations, the total harmonic distortion values in the grid current were measured and presented in detail in Fig. 14 and Table 4.

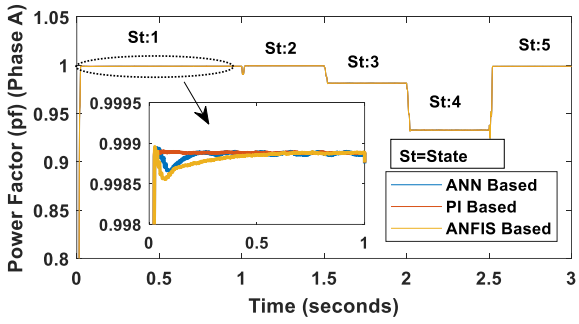

Figure 13. Effect of DC Link control methods on power factor

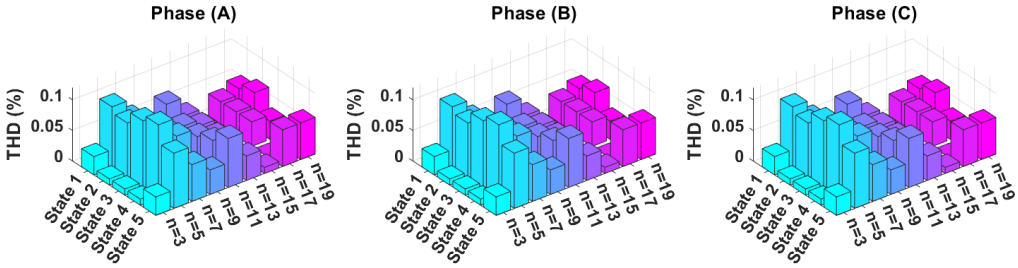

(a)

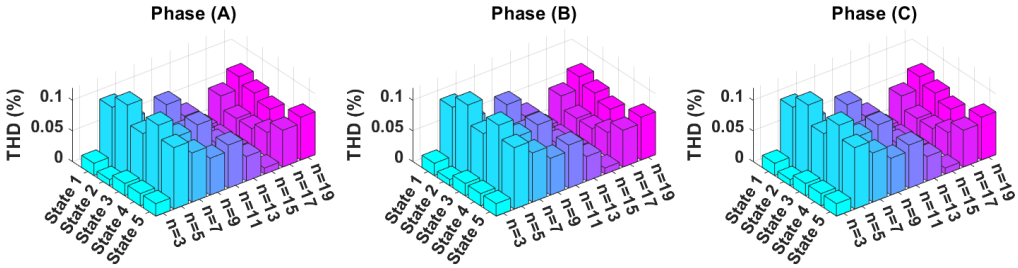

(b)

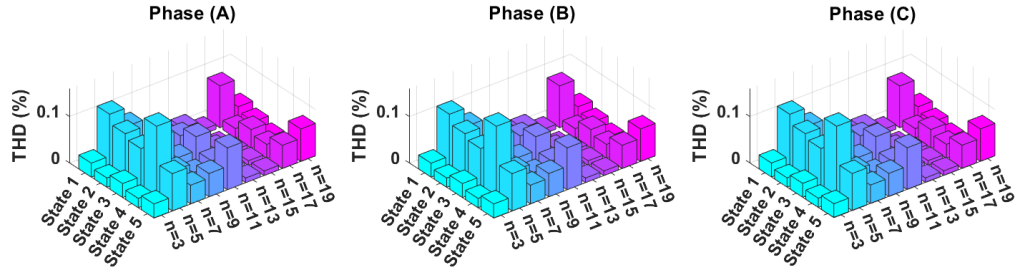

(c)

Figure 14. The effect of the proposed system on the harmonics in the grid current, Two closed loop pi (a) ANFIS (b) ANN (c)

Comparison of the harmonic distortion in the grid current in five different conditions of the system designed using a conventional inverter and a multilevel inverter is presented in Fig. 15. It is seen that the harmonic distortion performance of the multilevel inverter over the conventional inverter is superior in all conditions.

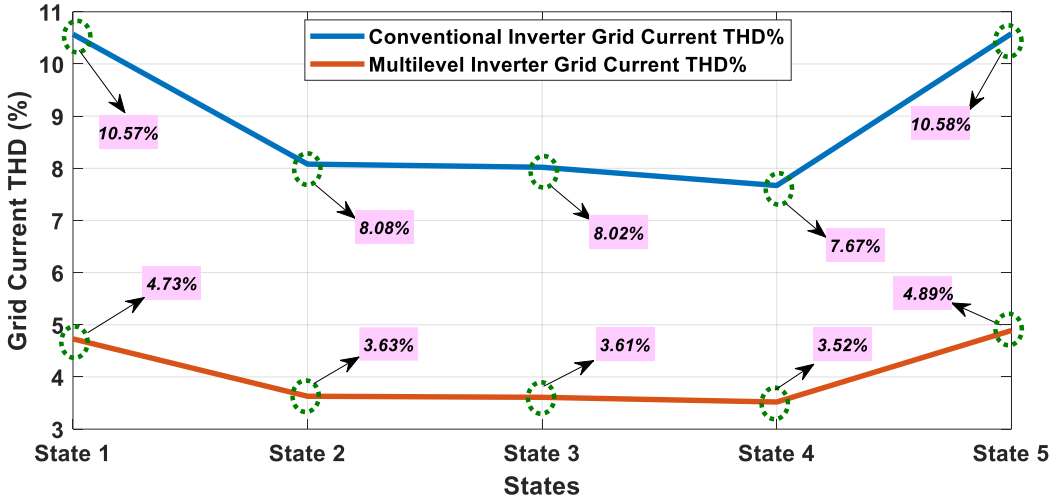

Figure 15. THD(%) performance of conventional and multilevel inverter

The effects of different dc-link control methods on active and reactive power control in five different operating states are shown in Fig. 16. It was observed that while active power fluctuations were <10w in pi-based closed-loop control, <15w in anfis-based control and <90w in ann control. In addition, detailed analysis results are presented in Table 4.

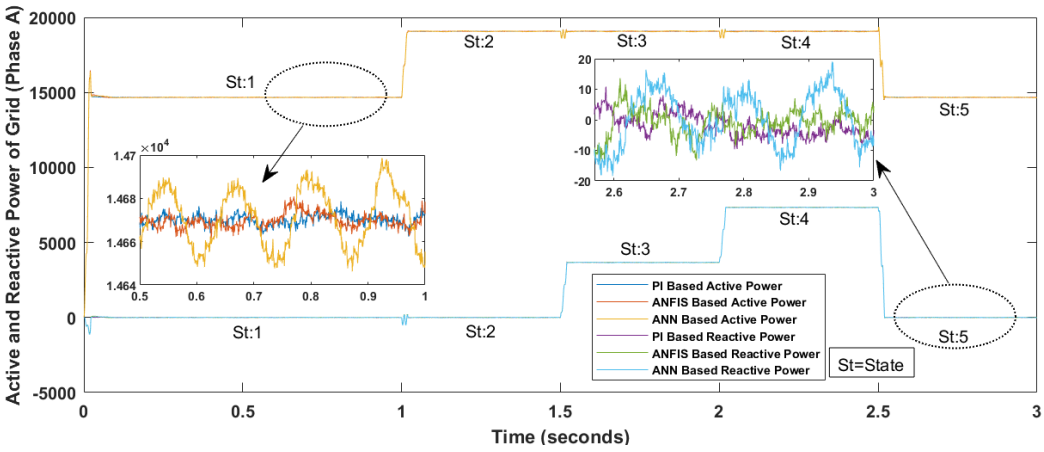

Figure 16. Active and reactive power fluctuations

PEMFC voltage, dc link voltage, power obtained from PEMFC, and duty cycle were analyzed under five different operating conditions. The data obtained by using different dc link control methods were examined. The DC link voltage is expected to be kept constant at 800 V and is used as the input voltage of the inverter. When DC link voltage control performance is compared in terms of convergence times, two closed-loop pi-based control methods show the best performance, while ANFIS-based control method shows the worst performance. In terms of DC link voltage fluctuation, the ANFIS-based control method outperformed the ANN-based control method. DC link voltage ripple, duty cycle, PEMFC power and voltage are detailed in Fig. 17 and Table 4.

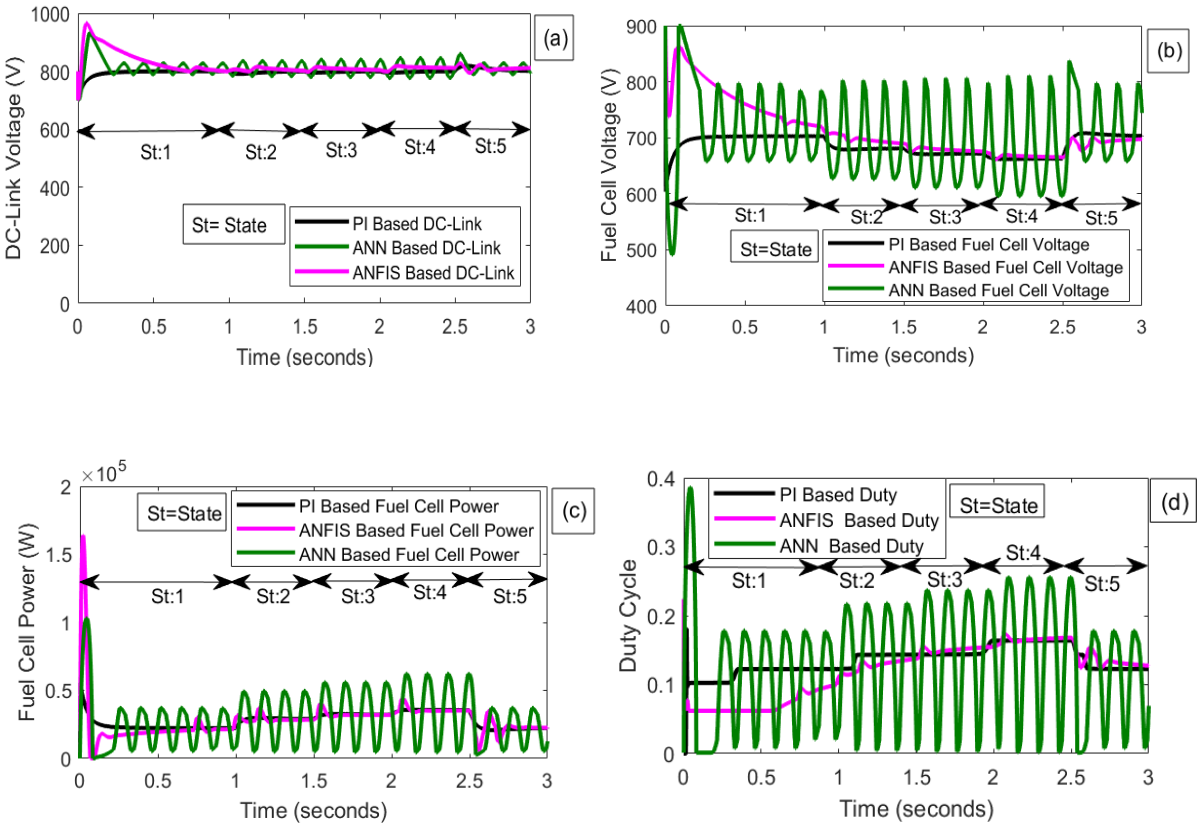

Figure 17. DC Link Voltage (a) Fuel Cell Voltage (b) Fuel Cell Power (c) Duty Cycle (d)

The effects of conventional inverter and multilevel inverter on power obtained from PEMFC under suddenly changing temperature (65°C-70°C) and performance conditions are presented in Fig. 18.

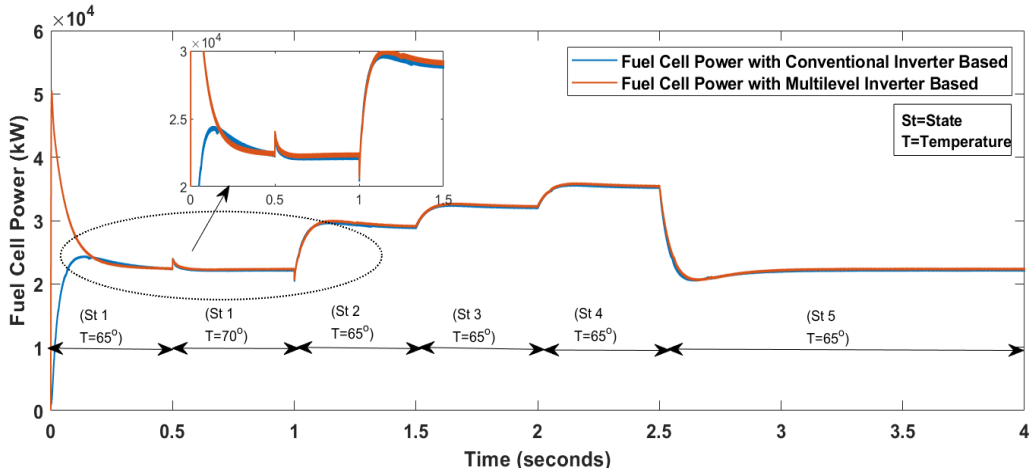

Figure 18. PEMFC power under different temperature and operational conditions

The system outputs of the proposed system and the operating conditions are presented in detail in Table 4.performances of the dc-link control methods in different

Table 4. Detailed presentation of system outputs

Operation States	DC Link Voltage Ripple (ΔV)	Power Fluctuaction (ΔP)	THD (Grid Current)	PF	Grid Power (Per Phase)	
					Active	Reactive

Two Closed Loop PI Based						
State 1	<1 V	9 W	4.73%	0.999	14.6 kW	0.003 kVAR
State 2	<1 V	9 W	3.63%	0.999	19 kW	0.002 VAR
State 3	<1 V	8 W	3.61%	0.981	19 kW	3.67 kVAR
State 4	<1 V	7 W	3.52%	0.932	19 kW	7.33 kVAR
State 5	<1 V	9 W	4.73%	0.999	14.6 kW	0.003 VAR
ANN						
State 1	27 V	50 W	4.76%	0.998	14.6 kW	0.01 kVAR
State 2	22 V	35 W	3.65%	0.999	19 kW	0.005 kVAR
State 3	26 V	60 W	3.61%	0.981	19 kW	3.68 kVAR
State 4	45 V	90 W	3.51%	0.932	19 kW	7.360 kVAR
State 5	27 V	50 W	4.76%	0.998	14.6 kW	0.01 kVAR
ANFIS						
State 1	12 V	15 W	4.83%	0.998	14.68 kW	0.005 kVAR
State 2	6 V	6 W	3.64%	0.999	19 kW	0.003 kVAR
State 3	7 V	6 W	3.61%	0.981	19 kW	3.67 kVAR
State 4	16 V	9 W	3.48%	0.932	19 kW	7.34 kVAR
State 5	12 V	15 W	4.83%	0.998	14.68kW	0.005 kVAR

Conclusion

In this study, efficient and low harmonic energy flow is tried to be provided for grid-connected PEMFC by using multi-level inverter and different dc link control methods (ANFIS, ANN, two closed loop based on pi). The multilevel inverter has outperformed conventional inverters in total harmonic distortion performance and complies with ieee-519 standards (<5%) (Figure 15, Table 4). In addition, the effects of dc link control methods on voltage and power fluctuations and total harmonic distortion are examined and presented in Fig. 10,16,17 and Table 4. In addition, while the minimum level of active and reactive power fluctuations is obtained in the anfis-based control method, the best result is obtained in the pi-based two closed-loop control method when the average power fluctuation performance is taken into account (Table 4). Based on the convergence time, the ANN-based control method performed better than the ampis-based control method (Fig. 17). In addition, this study has shown that even if the two closed-loop dc-link control methods based on pi have more advantageous points, finding the proportional and integral gain values is an effortful process. In addition, although multilevel inverters show higher performance than conventional inverters in terms of THD (%) and power factor, it is obvious that switching losses will be higher since more switching elements are used than conventional inverters. In addition, anfis and ann-based dc link control methods can be used with more input parameters and their performance can be improved with different learning methods. It is obvious that this study is also a candidate to be an alternative application for different renewable energy sources (wind, photovoltaic and etc.), grid connections of electric vehicles (vehicle to grid technology) and different power transfer systems.

Ethics committee approval and conflict of interest statement

"There is no need to obtain permission from the ethics committee for the article prepared" "There is no conflict of interest with any person / institution in the article prepared"

Authors' Contributions

Göncü B: Study conception and design, visualization, analysis, and interpretation of data, drafting of manuscript

Yılmaz Ü: supervised the project, critical revision

Acknowledgement

This study was supported by Harran University Scientific Research Projects Unit. Project Number: **22232**

References

[1] L. Sun, Y. Jin, L. Pan, J. Shen, K. Y. Lee, "Efficiency analysis and control of a grid-connected PEM fuel cell in distributed generation," *Energy Conversion and Management*, Vol. 195, pp. 587-596, 2019. https://doi.org/10.1016/j.enconman.2019.04.041

[2] M. Inci, "Active/reactive energy control scheme for grid-connected fuel cell system with local inductive loads," *Energy*,Vol. 197, 117191, pp.1-15, 2020. https://doi.org/10.1016/j.energy.2020.117191

[3] U. Yilmaz, O. Turksoy, "Artificial intelligence based active and reactive power control method for single-phase grid connected hydrogen fuel

cell systems," *International Journal of Hydrogen Energy*, Vol. 48, no. 21, pp. 7866-7883, 2023. https://doi.org/10.1016/j.ijhydene.2022.11.211

[4] N. Rasekh, M. Hosseinpour, "LCL filter design and robust converter side current feedback control for grid-connected Proton Exchange Membrane Fuel Cell system," *International Journal of Hydrogen Energy*, vol. 45, no. 23, pp. 13055-13067, 2020. https://doi.org/10.1016/j.ijhydene.2020.02.227.

[5] M. S. Kandil, M. M. El-Saadawi, A. E. Hassan and K. M. Abo-Al-Ez, "A proposed reactive power controller for DG grid connected systems," IEEE International Energy Conference, pp. 446-451, 2010. doi: 10.1109/ENERGYCON.2010.5771722

[6] Z. Maosong, Y. Cui, Q. Wang, J. Tao, X. Wang, H. Zhao, G Li. "A Study on Neutral-Point Potential in Three-Level NPC Converters," *Energies, vol.* 12, no. 3367, pp. 1-22, 2019. https://doi.org/10.3390/en12173367

[7] M. Kashif, M. J. Hossain, V. Sharma, S. M. Nawazish Ali and A. Khan, "Neutral-point Voltage Control of Three-level NPC Inverter for Three-phase APF based on Zero-sequence Voltage Injection," *International Conference on Electrical Engineering Research & Practice (ICEERP)*, pp. 1-5, 2019. doi: 10.1109/ICEERP49088.2019.8956988

[8] K.Tariq, M. Karabacak, V. S. Perić, S. Z. Hassan, L. M. Fernández-Ramírez. "Novel Improved Adaptive Neuro-Fuzzy Control of Inverter and Supervisory Energy Management System of a Microgrid," *Energies*, vol.13, no. 18, pp.1-20, 2020. https://doi.org/10.3390/en13184721

[9] A. H. Niasar, H. Moghbelli and A. Vahedi, "Adaptive Neuro-Fuzzy Control with Fuzzy Supervisory Learning Algorithm for Speed Regulation of 4-Switch Inverter Brushless DC Machines," *CES/IEEE 5th International Power Electronics and Motion Control Conference*, pp. 1-5, 2006. doi: 10.1109/IPEMC.2006.4778053

[10] K. K. Gupta and S. Jain, "A Novel Multilevel Inverter Based on Switched DC Sources," in *IEEE Transactions on Industrial Electronics*, vol. 61, no. 7, pp. 3269-3278, 2014. doi: 10.1109/TIE.2013.2282606

[11] K.B. Hamad, D.N. Luta, A.K. Raji , "A Grid-Tied Fuel Cell Multilevel Inverter with Low Harmonic Distortions," *Energies*. vol.14, no.3 pp.1-24, 2021. https://doi.org/10.3390/en14030688

[12] M.M. Savrun, M. İnci, "Adaptive neuro-fuzzy inference system combined with genetic algorithm to improve power extraction capability in fuel cell applications," *Journal of Cleaner Production*, vol. 299, 126944, pp. 1-11, 2021. https://doi.org/10.1016/j.jclepro.2021.126944

[13] P.K. Gayen, A. Jana, "An ANFIS based improved control action for single phase utility or micro-grid connected battery energy storage system," *Journal of Cleaner Production*, Volume 164; 1034-1049, 2017. https://doi.org/10.1016/j.jclepro.2017.07.007

[14] S. Yuvaraja, M. S. A. Salam, L. Vijayaraja, R. Kesavan, R. Dhanasekar, "A novel PWM scheme for grid-tied inverter in micro-grid with enhanced power quality using silicon cells," *Materials Today: Proceedings*, Volume 46, no 9, pp.4298-4304, 2021. https://doi.org/10.1016/j.matpr.2021.03.129

[15] A. Estebsari, S. Vogel, R. Melloni, M. Stevic, E. F. Bompard and A. Monti, "Frequency Control of Low Inertia Power Grids With Fuel Cell Systems in Distribution Networks," *IEEE Access*, vol. 10, pp. 71530-71544, 2022. doi:10.1109/ACCESS.2022.3187099

[16] K. B. Hamad, D. N. Luta., "PQ Open-Loop Control of a Grid-Tied Inverter Interfacing a Large-Scale Fuel Cell Stack.," *AIUE Proceedings of the 18th Industrial and Commercial Use of Energy Conference* 2020, pp 1-7., 2021, https://dx.doi.org/10.2139/ssrn.3735393

[17] C. Subhashree, S. K. Acharya, R. K. Khadanga, S. Mohanty, J. Arshad, A. U. Rehman, M. Shafiq, J.-G. Choi, "Harmonic Profile Enhancement of Grid Connected Fuel Cell through Cascaded H-Bridge Multi-Level Inverter and Improved Squirrel Search Optimization Technique," *Energies* vol.14, no. 23, pp.1-21 2021. https://doi.org/10.3390/en14237947

[18] W. Wang, B. Liu, Y. Hu, Z. Li, H. Wang, Y. Chen, S. Song, "Power Decoupling Control for Single-Phase Grid-Tied PEMFC Systems With Virtual-Vector-Based MPC," *in IEEE Access*, vol. 9, pp. 55132-55143, 2021. doi: 10.1109/ACCESS.2021.3071776

[19] M. R. Mahmud and H. R. Pota, "Robust Nonlinear Controller Design for DC–AC Converter in Grid-Connected Fuel Cell System," *in IEEE Journal of Emerging and Selected Topics in Industrial Electronics*, vol. 3, no. 2, pp. 342-351, 2022, doi: 10.1109/JESTIE.2021.3088394

[20] S. T. Meraj, N. Z. Yahaya, K. Hasan, M.S. H. Lipu, R.M. Elavarasan, A. Hussain, M.A. Hannan, K. M. Muttaqi, "A filter less improved control scheme for active/reactive energy management in fuel cell integrated grid system with harmonic reduction ability," *Applied Energy*,

vol. 312, 118784, 2022. https://doi.org/10.1016/j.apenergy.2022.118784

[21] M. Priya, P. Ponnambalam, ''Three-phase Grid Connected Modular-Multilevel Converter Fed by Proton Exchange Membrane Fuel Cell' *International Journal Of Renewable Energy Research*, vol. 12, no.1, pp. 466-478 2022 https://doi.org/10.20508/ijrer.v12i1.12802.g8420

[22] F. Vitale, N. Rispoli, M. Sorrentino, M.A. Rosen, C. Pianese, "On the use of dynamic programming for optimal energy management of grid-connected reversible solid oxide cell-based renewable microgrids," Energy, vol. 225, 120304, pp. 1-12, 2021, https://doi.org/10.1016/j.energy.2021.120304

[23] H. Li, B. Sun, J. Hao, J. Zhao, J. Li, A. Khakichi," Economical planning of fuel cell vehicle-to-grid integrated green buildings with a new hybrid optimization algorithm," *International Journal of Hydrogen Energy*, vol. 47, no. 13, pp. 8514-8531, 2022. https://doi.org/10.1016/j.ijhydene.2021.12.156.

[24] J. Jiang, R. Zhou, H. Xu, H. Wang, P. Wu, Z. Wang, J. Li, "Optimal sizing, operation strategy and case study of a grid-connected solid oxide fuel cell microgrid," *Applied Energy*, vol. 307, 2022, 118214, https://doi.org/10.1016/j.apenergy.2021.118214.

[25] M. Inci, "A flexible perturb & observe MPPT method to prevent surplus energy for grid-failure conditions of fuel cells," *International Journal of Hydrogen Energy*, vol. 46, no. 79, pp. 39483-39498, 2021. https://doi.org/10.1016/j.ijhydene.2021.09.185

[26] S.A. Saadat, S.M. Ghamari, H. Mollaee, F. Khavari, "Adaptive neuro-fuzzy inference systems (ANFIS) controller design on single-phase full-bridge inverter with a cascade fractional-order PID voltage controller," *IET Power Electron.*, vol.14, pp.1960–1972 2021. https://doi.org/10.1049/pel2.12162

[27] S. V. S. R. Pavankumar, S. Krishnaveni, Y. B. Venugopal and Y. S. K. Babu, "A Neuro-fuzzy Based Speed Control of Separately Excited DC Motor," *2010 International Conference on Computational Intelligence and Communication Networks*, Bhopal, India, pp. 93-98, 2010. doi: 10.1109/CICN.2010.132

[28] Lv, C., Xing, Y., Zhang, J., Na, X., Li, Y., Liu, T., Cao, D., & Wang, F. "Levenberg–Marquardt Backpropagation Training of Multilayer Neural Networks for State Estimation of a Safety-Critical Cyber-Physical System," *IEEE Transactions on Industrial Informatics*, vol. 14, no. 8, pp. 3436-3446, 2018. doi: 10.1109/TII.2017.2777460

[29] O. Rabiaa, B. H. Mouna, S. Lassaad, F. Aymen and A. Aicha, "Cascade Control Loop of DC-DC Boost Converter Using PI Controller," *2018 International Symposium on Advanced Electrical and Communication Technologies (ISAECT)*, pp. 1-5, 2018, doi: 10.1109/ISAECT.2018.8618859

[30] M. Kashif, M. J. Hossain, V. Sharma, S. M. Nawazish Ali and A. Khan, "Neutral-point Voltage Control of Three-level NPC Inverter for Three-phase APF based on Zero-sequence Voltage Injection," *International Conference on Electrical Engineering Research & Practice (ICEERP)*, pp. 1-5, 2019, doi: 10.1109/ICEERP49088.2019.8956988

[31] O. Turksoy, U. Yilmaz, Ahmet Teke, "Efficient AC-DC power factor corrected boost converter design for battery charger in electric vehicles," *Energy*, vol. 221, 119765, pp.1-18, 2021 https://doi.org/10.1016/j.energy.2021.119765

[32] U. Yilmaz, A. Kircay and S. Borekci, "PV system flyback converter controlled PI control to charge battery under variable temperature and irradiance," *Electronics*, Palanga, Lithuania, pp. 1-6, 2017. doi: 10.1109/ELECTRONICS.2017.7995223

[33] P. Jin-Hyuk, K.-B. Lee, "Performance Improvement for Reduction of Resonance in a Grid-Connected Inverter System Using an Improved DPWM Method" *Energies*, vol. 11, no. 113, pp.1-16, 2018. https://doi.org/10.3390/en11010113

[34] M. Milosevic, "Decoupling Control of d and q Current Components in Three-Phase Voltage Source Inverter," pp. 1-11 https://citeseerx.ist.psu.edu/viewdoc/download?doi=10.1.1.545.8150&rep=rep1&type=pdf

[35] B. Ren, X. Sun, S. An, X. Cao, Q. Zhang, "Analysis and design of an LCL filter for the three-level grid-connected inverter," *Proceedings of The 7th International Power Electronics and Motion Control Conference*, pp. 2023-2027, 2012. doi: 10.1109/IPEMC.2012.6259152